


Adaptive Photosensitizers **Hot Paper**
How to cite: *Angew. Chem. Int. Ed.* **2020**, *59*, 11779–11783

International Edition: doi.org/10.1002/anie.202000338

German Edition: doi.org/10.1002/ange.202000338

Constructing Adaptive Photosensitizers via Supramolecular Modification Based on Pillararene Host–Guest Interactions

 Li Shao⁺, Yutong Pan⁺, Bin Hua, Shidang Xu, Guocan Yu, Mengbin Wang, Bin Liu,^{*} and Feihe Huang^{*}

Abstract: In order to promote the development of photodynamic therapy (PDT), undesired side effects like low tumor specificity and the “always-on” phenomenon should be avoided. An effective solution is to construct an adaptive photosensitizer that can be activated to generate reactive oxygen species (ROS) in the tumor microenvironment. Herein, we design and synthesize a supramolecular switch based on a host–guest complex containing a water-soluble pillar[5]arene (WP5) and an AIEgen photosensitizer (G). The formation of the host–guest complex WP5⊃G quenches the fluorescence and inhibits ROS generation of G. Benefitting from the pH-responsiveness of WP5, the binding site between G and WP5 changes in an acidic environment through a shuttle movement. Consequently, fluorescence and ROS generation of the host–guest complex can be switched on at pH 5.0. This work offers a new paradigm for the construction of adaptive photosensitizers by using a supramolecular method.

Photodynamic therapy (PDT), which relies on photosensitizers and light for the generation of reactive oxygen species (ROS) to kill cancer cells or bacteria, has attracted much attention not only in fundamental research but also in clinical treatments.^[1] Compared with other traditional treatments, PDT possesses some unique advantages, such as spatiotemporal selectivity, high efficiency, no drug resistance, non-invasiveness and so on.^[2] In spite of these advantages, PDT

also shows some inevitable drawbacks hindering its development in preclinical and clinical investigations. For example, most photosensitizers possess some unwanted properties like dark toxicity, low water-solubility and photobleaching effects.^[3] Moreover, other undesired side effects of traditional PDT include the “always-on” model and low tumor specificity, which require patients to remain in the dark for a long period (usually a few weeks) following treatments.^[4] To overcome these disadvantages, developing adaptive photosensitizers with switchable photosensitizing effects is urgently required.

A general strategy to construct adaptive photosensitizers is to add quenchers or energy acceptors to the adjacent photosensitizers covalently, or accumulate a high number of photosensitizers in one polymeric backbone to induce self-quenching at a suitable density, which can be triggered in response to various stimuli at tumor sites.^[5] Although the direct covalent decoration has been proven to be an efficient and achievable method, it is impeded by the complicated molecular design, time-consuming synthesis, high cost and unwanted toxicity.^[6] Herein, we report a new strategy to construct adaptive photosensitizers via supramolecular modification based on pillararene host–guest interactions.^[7] Very specifically, we design and synthesize a supramolecular ROS switch based on a host–guest complex between an anionic water-soluble pillar[5]arene (WP5) host and a tetraphenylethene containing photosensitizer (G) guest (Scheme 1). This

[*] L. Shao,^[†] B. Hua, M. Wang, F. Huang

State Key Laboratory of Chemical Engineering, Center for Chemistry of High-Performance & Novel Materials, Department of Chemistry Zhejiang University

Hangzhou 310027 (P. R. China)

E-mail: fhuang@zju.edu.cn

Y. Pan,^[†] S. Xu, B. Liu

Department of Chemical and Biomolecular Engineering National University of Singapore

4 Engineering Drive 4, 117585 Singapore (Singapore)

E-mail: cheliub@nus.edu.sg

G. Yu

Laboratory of Molecular Imaging and Nanomedicine, National

Institute of Biomedical Imaging and Bioengineering

National Institutes of Health

Bethesda, MD 20892 (USA)

F. Huang

Green Catalysis Center and College of Chemistry

Zhengzhou University

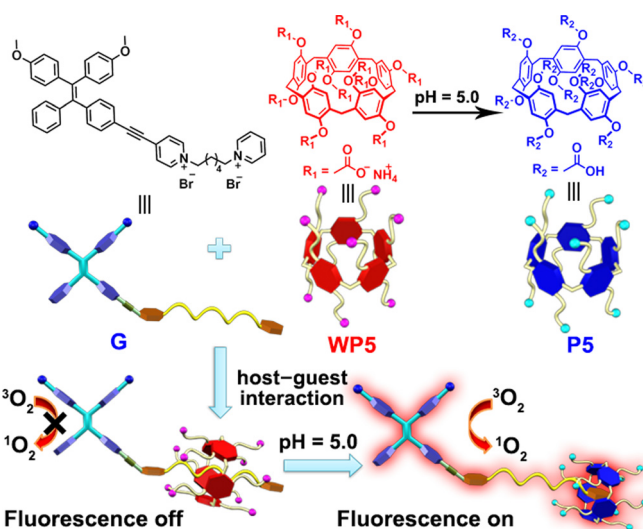
Zhengzhou 450001 (P. R. China)

[†] These authors contributed equally to this work.

 Supporting information and the ORCID identification number(s) for

 the author(s) of this article can be found under:

<https://doi.org/10.1002/anie.202000338>.

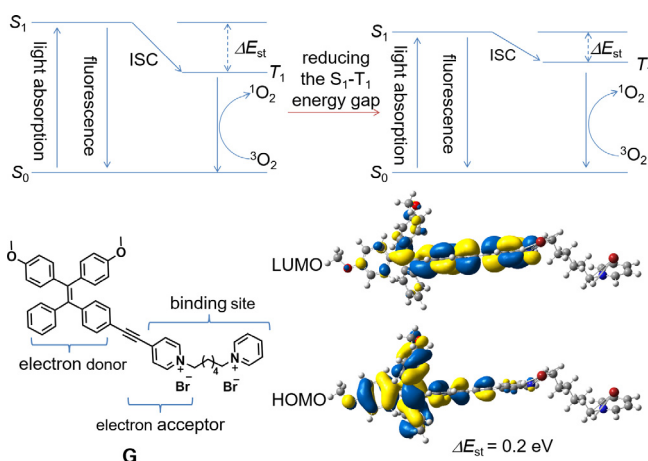


Scheme 1. Chemical structures and cartoon representations of WP5, P5 and G.

switch generates negligible fluorescence and ROS in neutral environments, but under acidic conditions, it displays bright red fluorescence and strong ROS generation ability. Considering that the tumors are acidic, the supramolecular ROS switch has potential as precision medicine for cancer treatment.

In order to construct supramolecular photosensitizers with switchable photosensitizing, a photosensitizer unit with good ROS generation ability was required. Herein, an AIEgen-based photosensitizer **G** was synthesized. As shown in Scheme 2, **G** is composed of three parts: a propeller-shaped tetraphenylethene (TPE) fluorogen, an electron deficient pyridinium unit, and a hexyl chain with another pyridinium unit at the end. The TPE part not only endows **G** with aggregation-induced emission (AIE) properties but also serves as an electron donor. By combining the TPE electron donor with the pyridinium electron acceptor, the HOMO and LUMO distributions of **G** can be separated and the energy gap (ΔE_{st}) between the S_1 and T_1 state will be reduced (Scheme 2).^[8] As predicted by time-dependent density functional theory (TD-DFT), **G** has a small overlap between HOMO and LUMO with a low ΔE_{st} value of 0.2 eV, indicating a high intersystem crossing (ISC) rate for efficient ROS generation.^[8b,9] Besides, the hexyl chain with two pyridinium units at the end promotes the water solubility of **G** and also affords a binding site for **WP5** to form host-guest complex **WP5**⊃**G**.

Next, the ROS generation ability of **G** was investigated by using 9,10-anthracenediyl-bis(methylene)dimalonic acid (**ABDA**) as ROS indicator. The higher **ABDA** consumption means stronger ROS productivity and most likely higher photodynamic therapy efficacy. As expected, **G** has a strong ROS productivity, even higher than commercially used photosensitizer **Ce6**. As shown in Figure 1a and S4 in the Supporting Information, the consumption of **ABDA** was calculated to be 4.5 nmol in the presence of **G** upon irradiation for 140 s, while that of **Ce6** was 1.7 nmol in 300 s (Figure 1a and S5). Furthermore, the light cytotoxicity of **G**



Scheme 2. Energy diagram of conventional photosensitizers, the proposed strategy for improving 1O_2 generation, chemical structure and HOMO–LUMO distributions of **G**. The HOMO–LUMO distributions of **G** were calculated by TD-DFT (Gaussian 09/B3LYP/6-31G(d)).

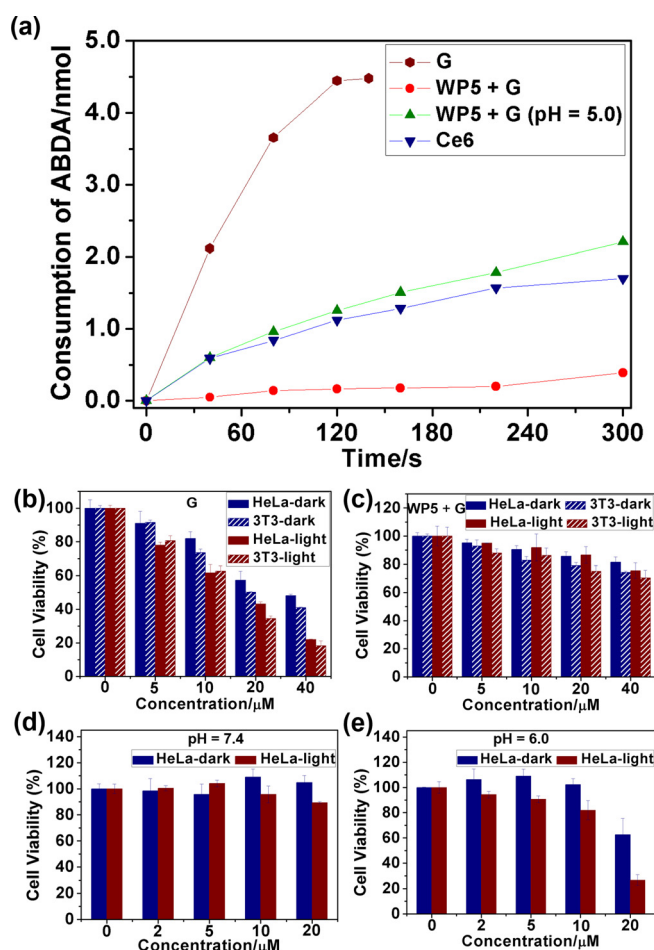


Figure 1. a) Consumption of **ABDA** (5.0 nmol) in the presence of **G** (30 μM), **Ce6** (30 μM), **WP5** (30 μM) and **G** (30 μM) and **WP5** (30 μM) and **G** (30 μM) at pH 5.0 under light irradiation (deducting the photobleaching of **ABDA**). Cell viability assay: b) **G** treated HeLa and 3T3 cells in dark and with the white light irradiation at a power density of 66 mWcm^{-2} for 10 min; c) **WP5** and **G** treated HeLa and 3T3 cells in dark and with the white light irradiation at a power density of 66 mWcm^{-2} for 10 min; **WP5** and **G** treated HeLa cells in PBS buffer at d) pH 7.4 and e) pH 6.0 in dark and with the white light irradiation at a power density of 66 mWcm^{-2} for 10 min.

was evaluated using 3-(4',5'-dimethylthiazol-2'-yl)-2,5-diphenyl tetrazolium bromide (MTT) assay under light irradiation. As shown in Figure 1b, the viability of HeLa and 3T3 cells was measured to be about 21% and 18% after incubation with 40 μM of **G** upon irradiation at a power density of 66 mWcm^{-2} for 10 min, indicating that **G** itself shows high light-toxicity to cancer cells. Notably, **G** also exhibited obvious cytotoxicity in the dark. As shown in Figure 1b, the cell viability decreased to be about 48% for HeLa cells and 40% against 3T3 normal cells at a concentration of 40 μM . The dark cytotoxicity may arise from the two pyridinium cations.

Interestingly we found that the complexation of **G** by **WP5** can efficiently inhibit the dark cytotoxicity. As shown in Figure 1c, the dark cytotoxicity of **G** decreased obviously after complexing with **WP5**. The cell viability retained about 80% for HeLa and 75% for 3T3 cells even under incubation

at a concentration of 40 μM **WP5** and 40 μM **G** for 24 hours. Moreover, compared with that of individual **G**, the ROS generation ability of **WP5** \supset **G** in aqueous media was very weak. As shown in Figure 1 a and S6, it was calculated that about 0.4 nmol **ABDA** was consumed under the white-light irradiation for 5 min. The light cytotoxicity of **G** in the presence of **WP5** was also determined. As shown in Figure 1 c, the cell viability was still above 70% for both HeLa and 3T3 cells after incubating with 40 μM **WP5** and 40 μM **G** upon irradiation at a power density of 66 mW cm^{-2} for 10 min. Considering that both the dark and light cytotoxicity decreased, this system potentially overcomes the “always on” phenomenon and reduces the damage to normal tissue. Thus, an ROS switch with an “off” state was constructed.

We further tested whether the ROS productivity could be recovered with specific stimuli. It is well-known that percarboxylate pillar[5]arenes possess pH-responsiveness because the carboxylate group can be protonated in an acidic environment, resulting in the change of water solubility.^[10] Based on this, the ROS generation ability of **WP5** and **G** at pH 5.0 was measured under the same conditions mentioned before. We found that the ROS generation of **WP5** and **G** at pH 5.0 was much higher compared with that in a neutral environment. The consumption of **ABDA** was calculated to be 2.2 nmol in 300 s (Figure 1 a and S7), even higher than that of **Ce6**. From this, we can conclude that the ROS switch was turned on at pH 5.0. The cytotoxicity of **WP5** \supset **G** under different pH was evaluated to check whether this switch would work in vitro or not. HeLa cells were incubated in acidic PBS buffer to simulate the tumor site. It is notable that the pH of acidic PBS buffer was adjusted to 6.0 rather than 5.0, as the cells will be inactivated at pH 5.0. As shown in Figure 1 d and 1e, dark cytotoxicity of **WP5** and **G** toward HeLa cells incubated in PBS buffer with different pH values was not very high even if the concentration reached 20 μM . Interestingly, remarkable light cytotoxicity of **WP5** and **G** toward HeLa cells was observed at 20 μM in PBS buffer with a pH value of 6.0. The viability of HeLa cells was measured to be about 26% at pH 6.0, much lower than that at pH 7.4 ($\approx 89\%$). That is, the “on” switch-state with high potential for photodynamic therapy was obtained in the acidic environment.

More interestingly, the fluorescence of **WP5** \supset **G** was also pH responsive. As shown in Figure 2 a, the AIE molecule **G** itself showed very weak fluorescence in aqueous solution because of its good water-solubility. Negligible change in fluorescence was observed after addition of **WP5** to the solution of **G** or acidification of the aqueous solution of **G** itself to pH 5.0. If the solution of **WP5** and **G** was adjusted to the acidic environment (pH 5.0), the fluorescence was increased remarkably, as shown in Figure 2 b. The pH-titration experiment (pH ranging from 7.8 to 5.0) revealed that the fluorescence was increased rapidly when the pH was below 6.0 (Figures 2 b and S8), and it kept increasing until the solution-pH reached 5.0. As the tumor tissue is relatively acidic, this phenomenon is very exciting because the acid-triggered switch can potentially light up the tumor site.^[11]

Furthermore, we tested whether the fluorescence of this ROS switch was preserved in cells and retained its pH-

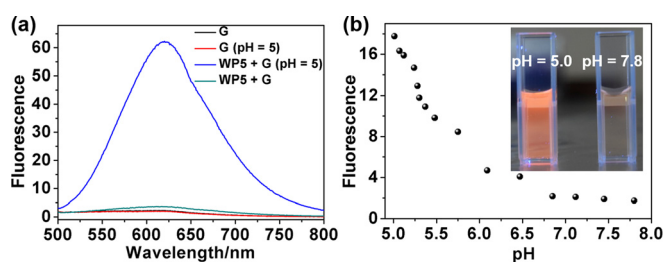


Figure 2. a) Fluorescence spectra of **G** (30 μM), **WP5** (30 μM) and **G** (30 μM), **G** (30 μM) at pH 5.0, and **WP5** (30 μM) and **G** (30 μM) at pH 5.0. b) Solution pH dependence of the fluorescence intensity of **WP5** and **G** in aqueous solution at 620 nm. Inset: Photograph of the mixture solutions of **WP5** (30 μM) and **G** (30 μM) in different pH conditions under a UV-lamp (365 nm).

responsiveness. Considering that lysosome has an acidic environment (at a pH about 5.0), **WP5** \supset **G** should accumulate in lysosome and emit red fluorescence after endocytosis. Confocal laser scanning microscopy experiments were conducted to verify this hypothesis. HeLa cells were incubated with **WP5** and **G** for 3 hours, and then Lyso-Tracker Green DND-26 was used to label the lysosomes. As expected, the fluorescence of **WP5** \supset **G** overlaps well with the fluorescence from Lyso-Tracker (Figure 3 a–c). The cell imaging experiments in buffer solutions with pH values of 7.4, 6.0 and 5.0 were also conducted (Figure S9), which indicated that the host–guest complex was stable in cells and retains its pH-responsiveness.

The mechanism of the changes in ROS generation and the pH-responsive fluorescence were further investigated. The overall features of **G**, **WP5** \supset **G** and **WP5** \supset **G** (pH 5.0) are shown in Scheme 3. First, the complexation between **WP5** and **G** was studied by ^1H NMR spectroscopy. The signals from **G** were identified clearly based on its 2D ^1H - ^1H COSY NMR spectrum (Figure S10). The proton signals of the alkyl chain and pyridinium parts on **G** shifted upfield significantly after addition of **WP5** (Figure S11b). NOE signals between protons on the alkyl chain part of **G** and **WP5** were observed (Figure S12), indicating that the alkyl chain was threaded into the cavity of **WP5**. Electrostatic interactions existed between the carboxylic anions on both the rims of **WP5** and the pyridinium cations on **G**, resulting in a [2]pseudorotaxane structure (Scheme 3). Photoinduced electron transfer (PET)

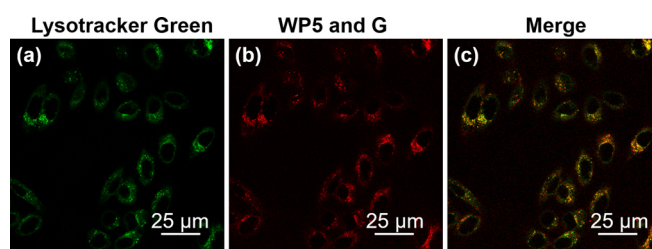
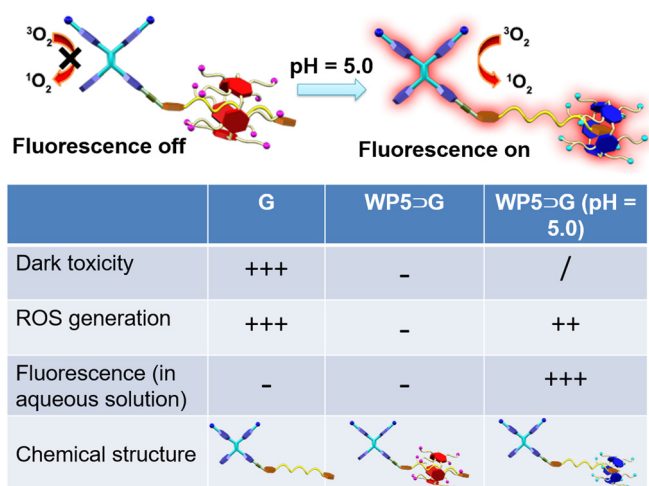


Figure 3. Colocalization of **WP5** and **G** with Lyso-Tracker Green DND-26 that labels lysosomes in HeLa cells: a) confocal image of 100 nM Lyso-Tracker Green (λ_{ex} : 500 nm/ λ_{em} : 510–600 nm); b) confocal image of 10 μM **WP5** and 10 μM **G** (λ_{ex} : 405 nm/ λ_{em} : 570–700 nm); c) the overlay image of (a) and (b).



Scheme 3. Complex models under different pH values and table of the dark toxicity, ROS generation and fluorescence of **G**, **WP5⊃G** and **WP5⊃G** (pH 5.0). “+” means the high level; “-” means the low level; “/” means not being measured.

occurred between **WP5** and **G**, resulting in the annihilating of ROS generation (Figure S13).^[3c] After adjusting the solution to pH 5.0, **WP5** was protonated to the neutral **P5** in acidic solution. As reported before, **P5** was expected to slip out of the alkyl chain part of **G** and precipitate, leaving individual **G** dissolved in solution.^[12] However, the proton signals from **G** cannot be detected in the NMR spectrum at pH 5.0 (Figure S11d). We speculated that neutral **P5** moved to the endmost pyridinium unit and complexed with it through cation- π interactions, as previously observed in the crystal structure of a similar system (Figure S14).^[13] This speculation was supported by the 2D NOESY NMR spectrum of **P5** and **G**: only NOE signals between protons $H_{a1,a2}$ on the endmost pyridinium unit of **G** and proton H_1 on **P5** were observed (Figure S15), verifying that **P5** was moved to the endmost pyridinium unit after the pH decrease. Since the hydrophilic pyridinium group on **G** was enshrouded by hydrophobic **P5**, **G** and **P5** coprecipitated. The aggregated state of **G** will further arouse its AIE properties, resulting in the dramatical increase of the fluorescence. Moreover, the **P5** ring in this state was turned away from the TPE core, so that **G** was returned to the original state, leading to the recovery of the ROS generation. Moreover, the association constants of **WP5/P5** and **G** were also measured using isothermal titration calorimetry (Figure S16,17), which were high enough to form stable host-guest complexes. TEM images were acquired to observe the microscopic morphologies of **G**, **WP5⊃G** and **WP5⊃G** (pH 5.0). As shown in Figure S18, **G** self-assembled to vesicles in water. After the addition of **WP5**, the morphology was transformed to tiny nanoparticles. After adjusting the pH of the **WP5** and **G** solution to 5.0, the self-assembly products changed to large aggregates, which is in good agreement with the results discussed above.

In conclusion, a supramolecular switch was constructed based on the host-guest complexation between an AIE photosensitizer and a water soluble pillar[5]arene. Fluorescence spectroscopy, confocal microscopy and MTT experi-

ments were utilized to prove the switch on-off processes. The results demonstrate that this switch does not show fluorescence and ROS generation ability in its off-state under neutral conditions, but it shows bright red fluorescence and high ROS generation ability in the on-state in acidic environments. Moreover, this switch can selectively light up lysosomes, demonstrating that it can stably exist after endocytosis. As tumors are acidic, this switch, with good pH-responsiveness and stability, can potentially be applied in cancer imaging and therapy. We hope this work will inspire the further construction of supramolecular materials in the field including active targeting, controlled release, smart switches and so on.

Acknowledgements

This work was supported by the National Natural Science Foundation of China (21434005) and the fundamental research funds for the central universities.

Conflict of interest

The authors declare no conflict of interest.

Keywords: host-guest systems · molecular switches · photosensitizers · pillararenes · supramolecular chemistry

- [1] a) D. E. Dolmans, D. Fukumura, R. K. Jain, *Nat. Rev. Cancer* **2003**, *3*, 380; b) A. P. Castano, P. Mroz, M. R. Hamblin, *Nat. Rev. Cancer* **2006**, *6*, 535; c) J. P. Celli, B. O. Spring, I. Rizvi, C. L. Evans, K. S. Samkoe, S. Verma, B. W. Pogue, T. Hasan, *Chem. Rev.* **2010**, *110*, 2795; d) S. S. Lucky, K. C. Soo, Y. Zhang, *Chem. Rev.* **2015**, *115*, 1990; e) J. Li, D. Cui, Y. Jiang, J. Huang, P. Cheng, K. Pu, *Adv. Mater.* **2019**, *31*, 1905091; f) H. Huang, S. Banerjee, K. Qiu, P. Zhang, O. Blacque, T. Malcomson, M. J. Paterson, G. J. Clarkson, M. Staniforth, V. G. Stavros, G. Gasser, H. Chao, P. J. Sadler, *Nat. Chem.* **2019**, *11*, 1041–1048.
- [2] a) Á. Juarranz, P. Jaén, F. S. Rodríguez, J. Cuevas, S. González, *Clin. Transl. Oncol.* **2008**, *10*, 148; b) K. Kostovic, Z. Pastar, R. Ceovic, Z. B. Mokos, D. S. Buzina, A. Stanimirovic, *Coll. Antropol.* **2012**, *36*, 1477; c) M. Wu, W. Wu, Y. Duan, X. Li, G. Qi, B. Liu, *Chem. Mater.* **2019**, *31*, 7212; d) G. Qi, F. Hu, Kenry, L. Shi, M. Wu, B. Liu, *Angew. Chem. Int. Ed.* **2019**, *58*, 16229; *Angew. Chem.* **2019**, *131*, 16375.
- [3] a) A. Taniguchi, Y. Shimizu, K. Oisaki, Y. Sohma, M. Kanai, *Nat. Chem.* **2016**, *8*, 974; b) J. He, Y. Wang, M. A. Missinato, E. Onuoha, L. A. Perkins, S. C. Watkins, C. M. St Croix, M. Tsang, M. P. Bruchez, *Nat. Methods* **2016**, *13*, 263; c) J. Gao, J. Li, W.-C. Geng, F.-Y. Chen, X. Duan, Z. Zheng, D. Ding, D.-S. Guo, *J. Am. Chem. Soc.* **2018**, *140*, 4945; d) Y. Wang, W. Wu, J. Liu, P. N. Manghnani, F. Hu, D. Ma, C. Teh, B. Wang, B. Liu, *ACS Nano* **2019**, *13*, 6879.
- [4] a) J. Tian, J. Zhou, Z. Shen, L. Ding, J.-S. Yu, H. Ju, *Chem. Sci.* **2015**, *6*, 5969; b) Y. Wang, Y. Lin, H.-g. Zhang, J. Zhu, *J. Cancer Res. Clin. Oncol.* **2016**, *142*, 813; c) X. S. Li, S. Kolemen, J. Yoon, E. U. Akkaya, *Adv. Funct. Mater.* **2017**, *27*, 1604053.
- [5] a) Y. Yuan, C.-J. Zhang, M. Gao, R. Zhang, B. Tang, B. Liu, *Angew. Chem. Int. Ed.* **2015**, *54*, 1780; *Angew. Chem.* **2015**, *127*, 1800; b) Z. Zhou, J. Song, R. Tian, Z. Yang, G. Yu, L. Lin, G. Zhang, W. Fan, F. Zhang, G. Niu, L. Nie, X. Chen, *Angew. Chem. Int. Ed.* **2017**, *56*, 6492; *Angew. Chem.* **2017**, *129*, 6592; c) F. Hu,

- G. Qi, Kenry, D. Mao, S. Zhou, M. Wu, W. Wu, B. Liu, *Angew. Chem. Int. Ed.* **2019**, <https://doi.org/10.1002/anie.201910187>; *Angew. Chem.* **2019**, <https://doi.org/10.1002/ange.201910187>.
- [6] a) J. F. Lovell, T. Liu, J. Chen, G. Zheng, *Chem. Rev.* **2010**, *110*, 2839; b) L. Zhang, X. A. Liu, K. D. Gillis, T. E. Glass, *Angew. Chem. Int. Ed.* **2019**, *58*, 7611; *Angew. Chem.* **2019**, *131*, 7693.
- [7] a) K. Liu, Y. Liu, Y. Yao, H. Yuan, S. Wang, Z. Wang, X. Zhang, *Angew. Chem. Int. Ed.* **2013**, *52*, 8285; *Angew. Chem.* **2013**, *125*, 3888; b) L. Wang, L.-I. Li, Y.-s. Fan, H. Wang, *Adv. Mater.* **2013**, *25*, 3888; c) M. Zhang, X. Yan, F. Huang, Z. Niu, H. W. Gibson, *Acc. Chem. Res.* **2014**, *47*, 1995; d) X. Ma, Y. Zhao, *Chem. Rev.* **2015**, *115*, 7794; e) H. Bai, H. Yuan, C. Nie, B. Wang, F. Lv, L. Liu, S. Wang, *Angew. Chem. Int. Ed.* **2015**, *54*, 13208; *Angew. Chem.* **2015**, *127*, 13406; f) H. Bai, F. Lv, L. Liu, S. Wang, *Chem. Eur. J.* **2016**, *22*, 11114; g) X.-Q. Wang, Q. Lei, J.-Y. Zhu, W.-J. Wang, Q. Cheng, F. Gao, Y.-X. Sun, X.-Z. Zhang, *ACS Appl. Mater. Interfaces* **2016**, *8*, 22892; h) L. Rui, Y. Xue, Y. Wang, Y. Gao, W. Zhang, *Chem. Commun.* **2017**, *53*, 3126; i) T. Sarma, G. Kim, S. Sen, W.-Y. Cha, Z. Duan, M. D. Moore, V. M. Lynch, Z. Zhang, D. Kim, J. L. Sessler, *J. Am. Chem. Soc.* **2018**, *140*, 12111; j) X. Ji, M. Ahmed, L. Long, N. M. Khashab, F. Huang, J. L. Sessler, *Chem. Soc. Rev.* **2019**, *48*, 2682.
- [8] a) H. Uoyama, K. Goushi, K. Shizu, H. Nomura, C. Adachi, *Nature* **2012**, *492*, 234; b) S. Xu, Y. Yuan, X. Cai, C.-J. Zhang, F. Hu, J. Liang, G. Zhang, D. Zhang, B. Liu, *Chem. Sci.* **2015**, *6*, 5824; c) S. Xu, Y. Duan, B. Liu, *Adv. Mater.* **2019**, *31*, 1903530.
- [9] a) J. Li, T. Nakagawa, J. MacDonald, Q. Zhang, H. Nomura, H. Miyazaki, C. Adachi, *Adv. Mater.* **2013**, *25*, 3319; b) S. Y. Lee, T. Yasuda, Y. S. Yang, Q. Zhang, C. Adachi, *Angew. Chem. Int. Ed.* **2014**, *53*, 6402; *Angew. Chem.* **2014**, *126*, 6520; c) W. Wu, D. Mao, F. Hu, S. Xu, C. Chen, C.-J. Zhang, X. Cheng, Y. Yuan, D. Ding, D. Kong, B. Liu, *Adv. Mater.* **2017**, *29*, 1700548; d) W. Wu, D. Mao, S. Xu, M. Panahandeh-Fard, Y. Duan, F. Hu, D. Kong, B. Liu, *Adv. Funct. Mater.* **2019**, *29*, 1901791.
- [10] a) T. Ogoshi, T.-a. Yamagishi, Y. Nakamoto, *Chem. Rev.* **2016**, *116*, 7937; b) W. Feng, M. Jin, K. Yang, Y. Pei, Z. Pei, *Chem. Commun.* **2018**, *54*, 13626; c) K. Yang, J. Wen, S. Chao, J. Liu, K. Yang, Y. Pei, Z. Pei, *Chem. Commun.* **2018**, *54*, 5911; d) J. Wu, J. Tian, L. Rui, W. Zhang, *Chem. Commun.* **2018**, *54*, 7629; e) M. Hao, G. Sun, M. Zuo, Z. Xu, Y. Chen, X.-Y. Hu, L. Wang, *Angew. Chem. Int. Ed.* **2019**, <https://doi.org/10.1002/anie.201912654>; *Angew. Chem.* **2019**, <https://doi.org/10.1002/ange.201912654>.
- [11] a) K. Zhou, Y. Wang, X. Huang, K. Luby-Phelps, B. D. Sumer, J. Gao, *Angew. Chem. Int. Ed.* **2011**, *50*, 6109; *Angew. Chem.* **2011**, *123*, 6233; b) D. Chen, Q. Tang, J. Zou, X. Yang, W. Huang, Q. Zhang, J. Shao, X. Dong, *Adv. Healthcare Mater.* **2018**, *7*, 1701272; c) F. Li, Y. Du, J. Liu, H. Sun, J. Wang, R. Li, D. Kim, T. Hyeon, D. Ling, *Adv. Mater.* **2018**, *30*, 1802808; d) Z. Yang, W. Fan, W. Tang, Z. Shen, Y. Dai, J. Song, Z. Wang, Y. Liu, L. Lin, L. Shan, Y. Liu, O. Jacobson, P. Rong, W. Wang, X. Chen, *Angew. Chem. Int. Ed.* **2018**, *57*, 14101; *Angew. Chem.* **2018**, *130*, 14297.
- [12] a) N. Song, Y.-W. Yang, *Chem. Soc. Rev.* **2015**, *44*, 3474; b) M. Ni, N. Zhang, W. Xia, X. Wu, C. Yao, X. Liu, X.-Y. Hu, C. Lin, L. Wang, *J. Am. Chem. Soc.* **2016**, *138*, 6643; c) L. Jiang, X. Huang, D. Chen, H. Yan, X. Li, X. Du, *Angew. Chem. Int. Ed.* **2017**, *56*, 2655; *Angew. Chem.* **2017**, *129*, 2699; d) M. Zuo, W. Qian, Z. Xu, W. Shao, X.-Y. Hu, D. Zhang, J. Jiang, X. Sun, L. Wang, *Small* **2018**, *14*, 1801942.
- [13] L. Shao, B. Hua, J. Liu, F. Huang, *Chem. Commun.* **2019**, *55*, 4527.

Manuscript received: January 8, 2020
Revised manuscript received: April 14, 2020
Accepted manuscript online: April 23, 2020
Version of record online: May 12, 2020